marine drugs

MDPI

Article

Hemiacetalmeroterpenoids A–C and Astellolide Q with Antimicrobial Activity from the Marine-Derived Fungus *Penicillium* sp. N-5

Tao Chen, Wencong Yang, Taobo Li, Yihao Yin, Yufeng Liu, Bo Wang * and Zhigang She *

School of Chemistry, Sun Yat-sen University, Guangzhou 510275, China
* Correspondence: ceswb@mail.sysu.edu.cn (B.W.); cesshzhg@mail.sysu.edu.cn (Z.S.)

Abstract: Four new compounds including three andrastin-type meroterpenoids hemiacetalmeroterpenoids A-C (**1**–**3**), and a drimane sesquiterpenoid astellolide Q (**15**), together with eleven known compounds (**4**–**14**) were isolated from the cultures of the marine-derived fungus *Penicillium* sp. N-5, while compound **14** was first isolated from a natural source. The structures of the new compounds were determined by analysis of detailed spectroscopic data, and the absolute configurations were further decided by a comparison of the experimental and calculated ECD spectra. Hemiacetalmeroterpenoid A (**1**) possesses a unique and highly congested 6,6,6,6,5,5-hexa-cyclic skeleton. Moreover, the absolute configuration of compound **14** was also reported for the first time. Compounds **1**, **5** and **10** exhibited significant antimicrobial activities against *Penicillium italicum* and *Colletrichum gloeosporioides* with MIC values ranging from 1.56 to 6.25 μg/mL.

Keywords: andrastin-type meroterpenoids; drimane sesquiterpenoid; marine-derived fungus; antimicrobials activities

Citation: Chen, T.; Yang, W.; Li, T.; Yin, Y.; Liu, Y.; Wang, B.; She, Z. Hemiacetalmeroterpenoids A–C and Astellolide Q with Antimicrobial Activity from the Marine-Derived Fungus *Penicillium* sp. N-5. *Mar. Drugs* **2022**, *20*, 514. https://doi.org/10.3390/md20080514

Academic Editor: Dehai Li

Received: 1 August 2022
Accepted: 12 August 2022
Published: 13 August 2022

1. Introduction

Andrastins are meroterpenoids characterized by a 6,6,6,5-tetra-carbocyclic skeleton. They are biogenetically derived from 3,5-dimethylorsellinic acid (DMOA) and farnesyl diphosphate (FPP), synthesized via a mixed polyketide-terpenoid pathway, and usually possess a keto-enol tautomerism at the cyclopentane ring [1–4]. To date, over 40 andrastins have been reported with multiple potential biological activities, including cytotoxic [5], anti-inflammatory [6], antiproliferative [7] and antimicrobial activity [4]. The complex structures and potential biological activities of andrastins have attracted much attention in recent years [8–10].

Marine fungus is known to be a natural source of structurally diverse and biologically active metabolites for drug discovery [11–16]. Recently, a series of novel bioactive natural products from marine fungi were reported by our group [17–22]. In our ongoing search for new bioactive secondary metabolites from marine fungi, the fungus *Penicillium* sp. N-5, isolated from the rhizosphere soil of mangrove plant *Avicennia marina*, led to the isolation of four new compounds, hemiacetalmeroterpenoids A–C (**1**–**3**) and astellolide Q (**15**). Especially, hemiacetalmeroterpenoid A (**1**) was a new andrastin-type meroterpenoid containing a unique 6,6,6,6,5,5-hexa-cyclic skeleton. Meanwhile, eleven known compounds, including 3-deacetyl-citreohybridonol (**4**) [23] citreohybridone A (**5**) [24], 3,5-dimethylorsellinic acid-based meroterpenoid 2 (**6**) [5], andrastins A–C (**7**, **10**, **13**) [25], andrastone C (**8**) [26], penimeroterpenoid A (**9**) [4], 23-deoxocitreohybridonol (**11**) [1], 6α-hydroxyandrastin B (**12**) [1], and compound V (**14**) [27] were also obtained from the fungus N-5 (Figure 1). All the isolated compounds were investigated for their antimicrobial activity against two phytopathogenic fungi and four bacterial strains. Herein, we report the isolation, structural characterization and antibacterial activity of these compounds.

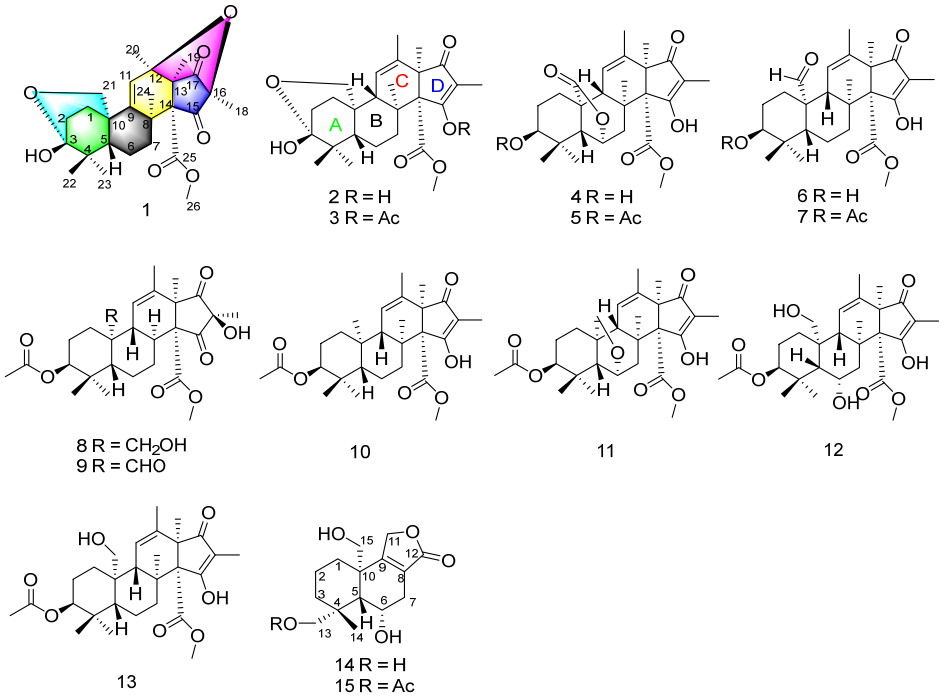

Figure 1. Structure of compounds **1**–**15**.

2. Results

2.1. Structure Identification

Hemiacetalmeroterpenoid A (**1**) was obtained as a white powder. It molecular formula was assigned as $C_{26}H_{34}O_7$ according to HRESIMS analysis at m/z 459.23709 $[M+H]^+$ (calcd. 459.23773), indicating ten degrees of unsaturation. In the ^{1}H NMR spectrum, the signal for one olefinic proton (δ_H 5.63), one methoxyl (δ_H 3.60), one methine (δ_H 1.47), four methylenes (δ_H 1.42, 1.62, 1.85, 1.91, 1.94, 2.11, 2.33 and 2.61) and six methyls (δ_H 1.03, 1.07, 1.19, 1.23, 1.33 and 1.49). The ^{13}C NMR data exhibited 26 carbon resonances, including two olefinic carbons for one double bond (δ_C 127.2, 150.1), three carbonyl carbons for two ketone (δ_C 203.7 and 203.8), and one ester carbonyl (δ_C 169.3), one methine (δ_C 49.1), five methylenes (one oxygenated), seven methyls (one oxygenated), eight quaternary carbons (one highly oxygenated: δ_C 99.8) (Table 1). The NMR data established a nucleus of meroterpenoid characterized by an andrastin scaffold, structurally similar to the citreohybriddione C (Figures S2 and S3) [28]. Analysis of the ^{1}H-^{1}H COSY data led to the identification of two isolated spin-systems of C-1/C-2 and C-5/C-6/C-7. The HMBC from H_2-1 to C-3, C-10, from H_1-5 to C-10, and from H_3-22 to C-3, C-4, C-5, C-23, ring A was formed. The HMBC correlations from H_3-24 to C-7, C-8, C-9, from H_1-11 to C-8, C-10 and from H_2-21 to C-5, C-10 completed ring B. Then, the HMBC cross-peaks from H_2-1, H_2-6 to C-10 and from H_3-23, H_2-7 to C-5 indicated ring A and ring B were fused at C-5 and C-10. Then, HMBC correlations from H_3-24 to C-14, C-15, from H_3-20 to C-11, C-12, C-13, C-17, from H_3-19 to C-12, C-13, C-14, C-17 and from H_3-18 to C-15, C-16, C-17, ring C and ring D were constituted, and they were blended at C-13 and C-14. The HMBC correlations from H_2-6, H_1-11 to C-8, from H_1-11 to C-10, suggested ring B and ring C were tightly connected. In addition, the HMBC correlation from H_3-26 to C-25 implied the presence of a methyl carboxylate. A weak HMBC correlation from H_3-26 to C-14 located the methyl carboxylate at C-14. Except one double bond, three carbonyls and four rings, ten degrees of unsaturation indicated that two new rings were required. According to the HMBC correlation from H_2-21 to C-3 (δ_C 99.8), a 6-membered ring was confirmed between C-1, C-2, C-3, C-10, and C-21. Finally, another new 5-membered ring was formed by intramolecular dehydration of hydroxyl groups at C-12 and C-16. Thus, the planar structure of **1** was established as shown in Figure 2.

Table 1. ^{1}H NMR (600 MHz) and ^{13}C NMR (150 MHz) of **1-3** in CD_3OD.

Position	1		2		3	
	δ_C	δ_H (*J* in Hz)	δ_C	δ_H (*J* in Hz)	δ_C	δ_H (*J* in Hz)
1	34.7 (CH_2)	1.42, m 2.33, m	35.3 (CH_2)	1.12, m 2.19, m	34.8 (CH_2)	1.15, m 2.20, m
2	30.2 (CH_2)	1.85, m 2.16, m	30.3 (CH_2)	1.74, m 2.12, m	30.1 (CH_2)	1.76, m 2.14, m
3	99.8 (C)		99.5 (C)		99.5 (C)	
4	41.4 (C)		41.3 (C)		41.3 (C)	
5	49.1 (CH)	1.47, m	50.9 (CH)	1.33, m	51.4 (CH)	1.21, m
6	19.4 (CH_2)	1.62, m 1.91, m	20.5 (CH_2)	1.55, m 1.75, m	20.4 (CH_2)	1.62, m 1.81, m
7	32.3 (CH_2)	1.94, m 2.61, m	32.5 (CH_2)	2.07, m 2.76, m	32.9 (CH_2)	1.94, m 2.23, m
8	40.2 (C)		42.4 (C)		41.9 (C)	
9	150.1 (C)		48.5 (CH)	1.89, t (2.7)	48.6 (CH)	1.98, t (2.7)
10	38.5 (C)		36.3 (C)		36.3 (C)	
11	127.2 (CH)	5.63, s	124.2 (CH)	5.42, m	126.0 (CH)	5.60, m
12	77.4 (C)		137.7 (C)		133.7 (C)	
13	54.4 (C)		57.5 (C)		60.6 (C)	
14	73.4 (C)		69.7 (C)		69.2 (C)	
15	203.7 (C)		190.7 (C)		171.9 (C)	
16	76.7 (C)		113.5 (C)		131.9 (C)	
17	203.8 (C)		201.4 (C)		202.1 (C)	
18	7.9 (CH_3)	1.19, s	6.6 (CH_3)	1.57, s	8.8 (CH_3)	1.55, s
19	11.0 (CH_3)	1.33, s	18.0 (CH_3)	1.18, s	17.4 (CH_3)	1.20, s
20	24.2 (CH_3)	1.23, s	20.2 (CH_3)	1.82, s	19.1 (CH_3)	1.75, s
21	74.4 (CH_2)	3.55, d (7.6) 4.39, d (8.7)	68.6 (CH_2)	3.81, d (9.0) 4.22, d (9.0)	68.5 (CH_2)	3.82, d (8.9) 4.21, d (9.0)
22	27.2 (CH_3)	1.07, s	27.9 (CH_3)	1.04, s	27.9 (CH_3)	1.07, s
23	18.9 (CH_3)	1.04, s	18.9 (CH_3)	1.01, s	18.8 (CH_3)	1.03, s
24	25.9 (CH_3)	1.49, s	16.7 (CH_3)	1.19, s	16.5 (CH_3)	1.24, s
25	169.3 (C)		172.6 (C)		170.9 (C)	
26	52.5 (CH_3)	3.60, s	51.9 (CH_3)	3.56,s	52.4 (CH_3)	3.59,s
Ac-CH_3					21.2 (CH_3)	2.36, s
Ac-OCO					167.3 (C)	

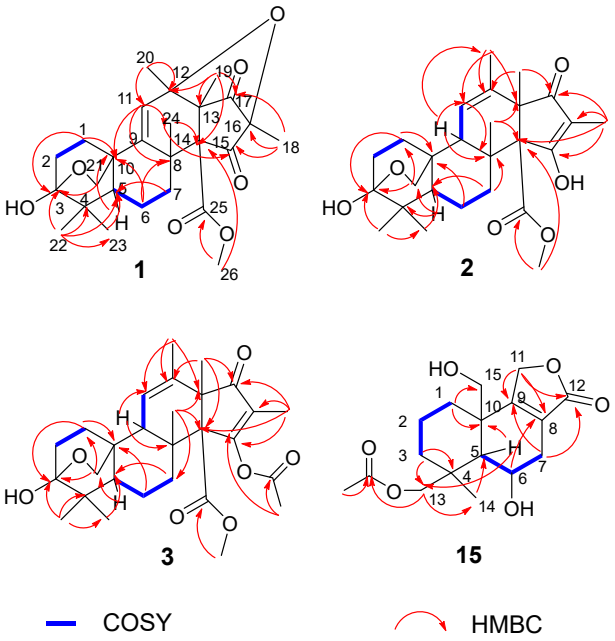

Figure 2. Key HMBC and COSY correlations of **1**–**3** and **15**.

The relative configuration of compound **1** was defined by the NOESY correlations. The correlations of H_2-21 with H_3-23, H_3-20 with H_3-19, H_3-24, and H_3-18 with H_3-19, H_3-26 were observed in the NOESY spectrum, which means H_3-18, H_3-19, H_3-20, H_2-21, H_3-23, H_3-24 and H_3-26 were on the same side. The NOESY correlations of H_1-5 with H_3-22 suggested that H_1-5 and H_3-22 were in the opposite face (Figure 3). The absolute configuration of **1** was determined by comparing the calculated ECD spectra generated by the time-dependent density functional theory (TDDFT) for two enantiomers 3*R*, 5*S*, 8*S*, 10*S*, 12*R*, 13*S*, 14*R*, 16*R*-**1a** and 3*S*, 5*R*, 8*R*, 10*R*, 12*S*, 13*R*, 14*S*, 16*S*-**1b** with the experimental one. Finally, the experimental ECD spectrum of **1** was nearly identical to the calculated ECD spectrum for **1a** (Figure 4), clearly suggesting the 3*R*, 5*S*, 8*S*, 10*S*, 12*R*, 13*S*, 14*R*, 16*R* absolute configuration for **1**.

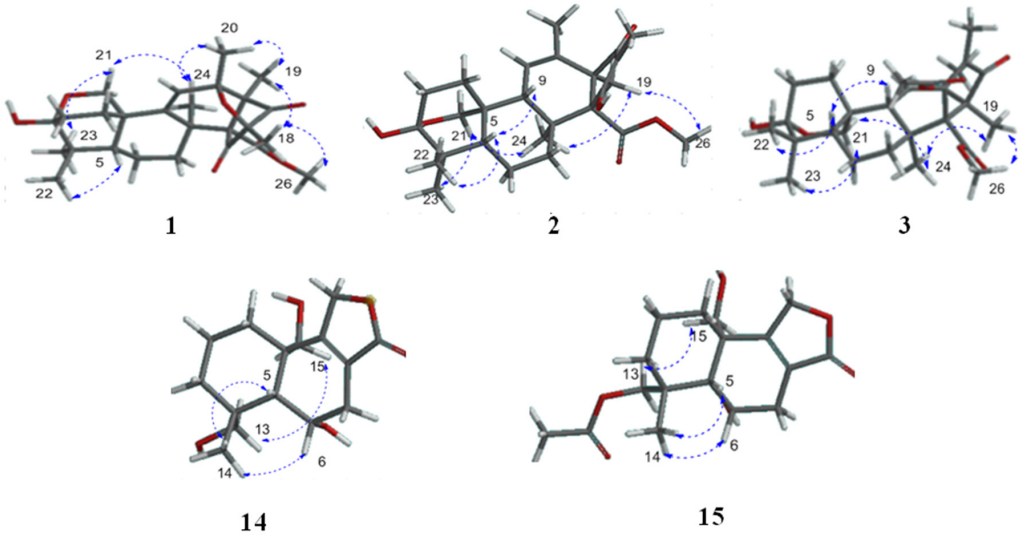

Figure 3. Key NOE correlations of **1**–**3** and **14**–**15**.

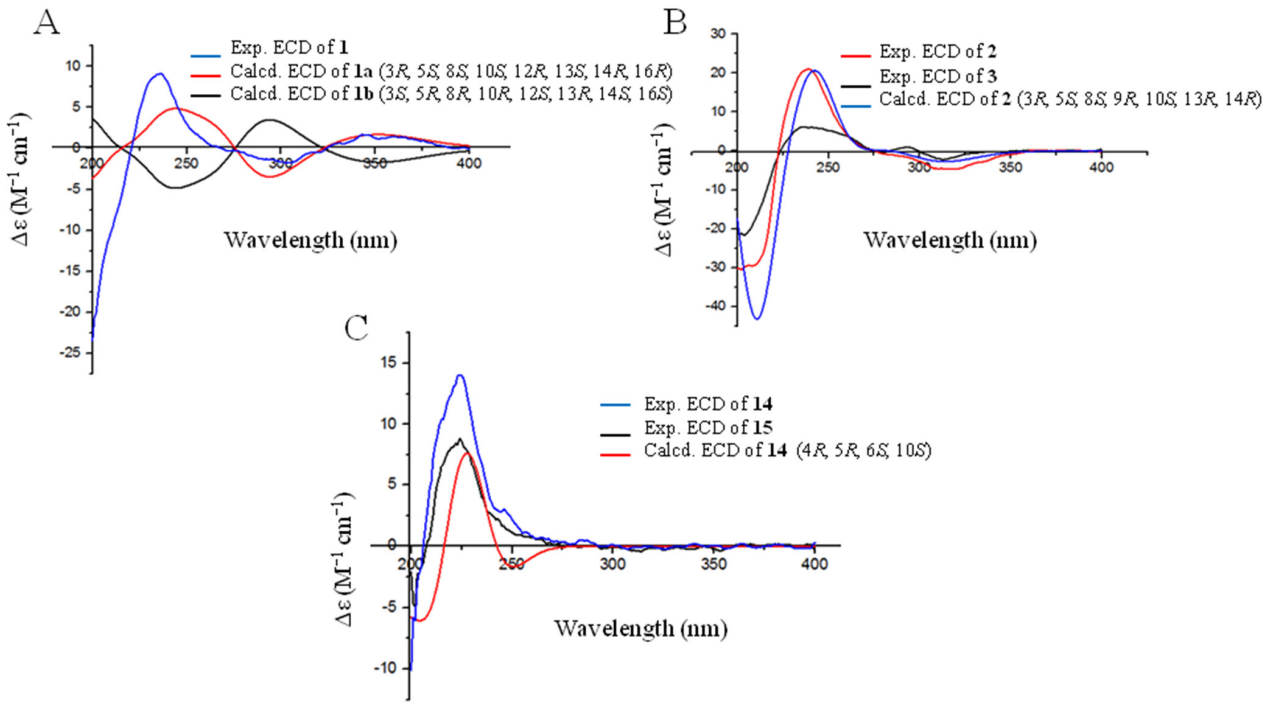

Figure 4. ECD spectra of compounds **1** (**A**), **2** and **3** (**B**), **14** and **15** (**C**) in CH_3OH.

Hemiacetalmeroterpenoid B (**2**) was isolated as a white powder and had a molecular formula of $C_{26}H_{36}O_6$, determined by HRESIMS data *m*/*z* 445.25772 $[M+H]^+$ (calcd. 445.25847) with nine degrees of unsaturation. The ^1H NMR spectrum of **2** displayed the signal for one olefinic proton (δ_H 5.42), one methoxyl (δ_H 3.56), two methines (δ_H 1.33 and 1.89), four methylenes (δ_H 1.12, 1.33, 1.55, 1.75, 2.07, 2.12, 2.19 and 2.76) and six methyls (δ_H 1.01, 1.04, 1.18, 1.19, 1.57 and 1.82). The ^{13}C NMR data revealed 26 carbon resonances, involving four olefinic carbons for two double bonds (δ_C 113.5, 124.2, 137.7, 190.7), two carbonyl carbons for one ketone (δ_C 201.4), one ester carbonyl (δ_C 172.6) (Table 1). According to 1D NMR and 2D NMR data, the planar structure of **2** was similar to the co-isolated andrastin B (**13**). The obvious difference is that the acetyl group at the C-3 position of compound **2** disappears. Meanwhile, the HMBC from H_2-21 to C-3 (δ_C 99.5) also indicated that a new 6-membered ring was formed between C-1, C-2, C-3, C-10 and C-21 (Figure 2).

The NOESY spectrum indicated that H_1-5, H_1-9 and H_3-22 were on the same side based on the correlations of H_1-5 with H_1-9 and H_3-22. On the contrary, it was suggested that H_3-19, H_3-21, H_3-23, H_3-24, and H_3-26 were on the other side based on the NOESY correlations of H_2-21 with H_3-23 and H_3-24, along with H_3-19 with H_3-24 and H_3-26 (Figure 3). Thus, the relative configuration of **2** was determined to be 3*R*, 5*S*, 8*S*, 9*R*, 10*S*, 13*R* and 14*R*. The absolute configuration of the stereogenic centers in **2** was assigned as 3*R*, 5*S*, 8*S*, 9*R*, 10*S*, 13*R* and 14*R* by comparing its experimental ECD spectrum with that of the calculated model molecule (Figure 4).

Hemiacetalmeroterpenoid C (**3**) was also purified as a white powder. The molecular formula was specified as $C_{28}H_{38}O_7$ (ten degrees of unsaturation) by HRESIMS (*m*/*z* 509.25015 $[M+Na]^+$), which is 42 mass units higher than that of **2** (Figure S17). Analysis of its NMR data (Table 1) revealed the presence of the same partial structure as that found in compound **2**. The only difference was **3** has an additional acetyl fragment. Finally, a weak HMBC correlation from Ac-CH_3 to C-15 suggested that the acetyl fragment was attached to C-15 (Figure 2).

Because compound **3** has the same chiral center as **2**, the NOESY correlation and experimental ECD spectrum of compound **3** were in agreement with those of **2** (Figures 3 and 4). Thus, the absolute configuration of **3** was identified as 3*R*, 5*S*, 8*S*, 9*R*, 10*S*, 13*R* and 14*R*.

Compound **14** was obtained as a yellow powder. Analysis of its ^1H NMR and ^{13}C NMR data showed that the planar structure of **14** was the same as compound V, which was the product of the alkaline hydrolysis of parasiticolide A [27]. However, the absolute configuration of compound V was ambiguous.

The relative configuration of **14** was also defined by the NOESY correlation. The correlations of H_3-14 with H_1-5 and H_1-6, and H_2-13 with H_2-15 were found in the NOESY spectrum, which means H_1-5, H_1-6, and H_3-4 were on the same side, and H_2-13 and H_2-15 were on the opposite face (Figure 3). Thus, the absolute configuration of the stereogenic centers in **14** was assigned as 4*R*, 5*R*, 6*S*, 10*S* by comparing its experimental ECD spectrum with that of the calculated model molecule (Figure 4). Finally, compound **14** was named as astellolide J.

Astellolide Q (**15**) was also acquired as a yellow powder. It molecular formula was determined as $C_{17}H_{24}O_6$ according to HRESIMS analysis at *m*/*z* 347.14578 $[M+Na]^+$ (calcd. 347.14651), indicating six degrees of unsaturation. The ^1H NMR of **15** showed two methyls (δ_H 1.15 and 2.08), four methylenes (δ_H 1.16, 1.45, 1.54, 1.78, 1.91, 2.05, 2.34 and 2.50), one methines (δ_H 1.74) one hydroxymethine (δ_H 4.55) and three hydroxy-methylenes (δ_H 3.34, 3.92, 4.09, 4.33, 4.84 and 5.04). In addition, according to the HSQC data, the ^{13}C NMR data showed the presence of 17 carbon signals, including two ester carbonyl carbons (δ_C 173.1, 177.0) and two olefinic carbons (δ_C 124.0, 169.0), one methyl, seven methylenes (three oxygenated), two methines (one oxygenated), two aliphatic quaternary carbons (Table 2). Analysis of its ^1H NMR and ^{13}C NMR data in association with the 2D NMR data established a nucleus of drimane sesquiterpenoid characterized by an astellolide scaffold, structurally similar to the co-isolated compound **14** (Figures S26 and S27). It can be clearly observed

that compound **15** has an additional acetyl fragment. Furthermore, the HMBC from H_2-13 to Ac-OCO indicated that the acetyl fragment was linked to C-13 (Figure 3).

Table 2. ^{1}H NMR (400 MHz) and ^{13}C NMR (100 MHz) of **15** in CD_3OD.

Position	δ_C	δ_H (*J* in Hz)	Position	δ_C	δ_H (*J* in Hz)
1	35.3 (CH_2)	1.45, m 2.05, m	10	44.2 (C)	
2	19.5 (CH_2)	1.54, m 1.78, m	11	71.8 (CH_2)	5.00, d (17.7) 4.84, d (17.6)
3	37.0 (CH_2)	1.16, m 1.91, m	12	177.0 (C)	
4	39.3 (C)		13	68.1 (CH_2)	4.44, d (11.2) 4.62, d (5.4)
5	56.4 (CH)	1.74, s	14	28.1 (CH_3)	1.16, s
6	63.6 (CH)	4.61, d (11.0)	15	65.7 (CH_2)	3.76, d (12.0) 4.33, d (11.9)
7	33.0 (CH_2)	2.34, d, (18.9) 2.50, d (18.3)	Ac-CH_3	20.8 (CH_3)	2.08, s
8	124.0 (C)		Ac-OCO	173.1 (C)	
9	169.0 (C)				

Finally, the NOESY correlation and experimental ECD spectrum of compound **15** were identical to those of **14** (Figures 3 and 4). Thus, the absolute configuration of **15** was also assigned as 4*R*, 5*R*, 6*S*, 10*S*.

2.2. Antimicrobial Assay

Compounds **1**–**15** were investigated for their antimicrobial activities against two phytopathogenic fungi and four bacterial strains. As shown in Table 3, andrastin-type meroterpenoids have better antimicrobial activities against phytopathogenic fungus than against bacteria. Most of all the tested compounds (9 compounds out of total 15 compounds) displayed potent antimicrobial activities (MIC < 50 μg/mL). Among them, compounds 1, 5 and 10 exhibited remarkable antimicrobial activities against *Penicillium italicum* and *Colletrichum gloeosporioides* with MIC values of 6.25, 1.56, 6.25 and 6.25, 3.13, 6.25 μg/mL. Moreover, compound 1 showed inhibitory activities against *Bacillus subtilis* under concentration of 6.25 μg/mL. Compound 10 also displayed significant antimicrobial activity against *Salmonella typhimurium* with an MIC value of 3.13 μg/mL. Notably, compound 5 revealed potential antimicrobial activity against all the strains, the MIC values were lower than 25 μg/mL.

Table 3. Antimicrobial activity of compounds **1**–**15**.

Microbial / Compound	Methicillin-Resistent *Staphyococcus aureus* (μg/mL) [a]	*Bacillus subtilis* (μg/mL) [a]	*Pseudomonas aeruginosa* (μg/mL) [a]	*Salmonella typhimurium* (μg/mL) [a]	*Penicillium italicum* (μg/mL) [a]	*Colletrichum gloeosporioides* (μg/mL) [a]
1	25	6.25	>50	>50	6.25	6.25
2	>50	>50	25	>50	50	>50
3	>50	>50	>50	>50	50	>50
4	>50	>50	>50	>50	>50	>50
5	50	25	25	>50	1.56	3.13
6	>50	25	50	>50	12.50	25
7	>50	>50	>50	>50	25	25
8	>50	>50	>50	>50	>50	>50
9	>50	>50	>50	>50	>50	>50

Table 3. *Cont.*

Compound \ Microbial	Methicillin-Resistent *Staphyococcus aureus* (μg/mL) [a]	*Bacillus subtilis* (μg/mL) [a]	*Pseudomonas aeruginosa* (μg/mL) [a]	*Salmonella typhimurium* (μg/mL) [a]	*Penicillium italicum* (μg/mL) [a]	*Colletrichum gloeosporioides* (μg/mL) [a]
10	25	12.50	25	3.13	6.25	6.25
11	>50	>50	>50	>50	>50	>50
12	>50	>50	>50	>50	>50	>50
13	50	>50	>50	>50	50	>50
14	>50	>50	>50	>50	>50	>50
15	>50	>50	>50	>50	25	25
Ampicillin	0.13	0.13	0.07	0.13	-	-
Ketoconazole	-	-	-	-	0.78	0.78

[a]: The deviation value of three parallel experiments; -: No test.

As for the study of the structure–activity relationship (SAR), it was found that the degree of oxidation at C-21 had different effects on the activities of the compounds. The compound with methyl (**10**) at C-21 has significantly antimicrobial activity, followed by the aldehyde group (**7**), and hydroxymethyl (**13**) was the weakest. In-depth analysis showed that apart from the degree of oxidation at C-21, keto-enol tautomerism at the cyclopentane ring also had obvious influences on the antimicrobial activities of compounds. Compared to compounds **7** and **13** (enol form), compounds **8** and **9** (keto form) showed no activities against all strains (Table 3).

3. Experimental Methods

3.1. General Experimental Procedures

The NMR were tested on a Bruker Avance 600 MHz spectrometer (Karlsruhe, Germany) at room temperature. Optical rotations data were recorded on an MCP300 (Anton Paar, Shanghai, China). UV were tested using a Shimadzu UV-2600 spectrophotometer (Shimadzu, Kyoto, Japan). IR spectra were recorded on IR Affinity-1 spectrometer (Shimadzu, Kyoto, Japan). HR-ESI-MS spectra were tested on a ThermoFisher LTQ-Orbitrap-LC-MS spectrometer (Palo Alto, CA, USA). LC-MS/MS data was performed on a Q-TOF manufactured by Waters and a Waters Acquity UPLC BEH C18 column (1.7 μm, 2.1 × 100 mm). Recoated silica gel plates (Qingdao Huang Hai Chemical Group Co., Qingdao, China, G60, F-254), Column chromatography (CC) and Sephadex LH-20 (Amersham Pharmacia, Stockholm, Sweden) were used to purify the compounds.

3.2. Fungal Material

Fungus N-5 was isolated from the rhizosphere soil of mangrove plant *Avicennia marina* (collected in October 2021 from Nansha Mangrove National Nature Reserve in Guangdong Province, China). It was identified as *Penicillum* sp. by the ITS region (deposited in GenBank, accession no ON926808), and fungus N-5 was deposited at Sun Yat-sen University, China.

3.3. Fermentation

The fungus *Penicillum* sp. N-5 was cultured in one hundred 1000 mL Erlenmeyer flasks at 25 °C for 30 days; these contained autoclaved rice solid-substrate medium composed of 50 g rice and 50 mL 3‰ saline water.

3.4. Extraction and Purification

After incubation, the mycelia and solid rice medium were extracted four times with EtOAc, and 75 g of residue was obtained. Next, the residue was separated by a gradient of petroleum ether/EtOAc from 9:1 to 0:10 (v/v) on silica gel CC and divided into six fractions (Fr.1–Fr.6). Fr. 2 (10 g) was separated to Sephadex LH-20 (methanol) to yield three sub-fractions (SFrs. 2.1–2.3). SFrs.2.3 (1.2 g) was applied to silica gel CC (DCM/MeOH v/v,

100:1) and further purified by reversed-phase (RP) high performance liquid chromatography (HPLC; 90–10% MeCN/H_2O for 25 min) to obtain compounds **1** (5 mg) and **3** (7 mg). Fr. 3 (16 g) was also separated to Sephadex LH-20 (methanol) to yield four sub-fractions (SFrs. 3.1–3.4). SFrs.3.1 (1.6 g) was separated to silica gel CC (DCM/MeOH *v*/*v*, 80:1) and further purified by reversed-phase (RP) high performance liquid chromatography (HPLC; 75–25% MeCN/H_2O for 22 min) to yield compounds **2** (11 mg) and **15** (6 mg).

Hemiacetalmeroterpenoid A (**1**): white powder, m.p. 122.8–124.1 °C; $[\alpha]_D^{25}$-52 (*c* 0.02, MeOH), UV (MeOH) λ_{max} (log ε): 206 (2.52) (Figure S33); ECD (MeOH) λ_{max} ($\Delta\varepsilon$): 240 (+5.47), 301 (−1.14), 362 (+0.61); ^{1}H (600 MHz, CD_3OD) and ^{13}C NMR (150 MHz, CD_3OD) data, see Table 1; HR-ESI-MS: *m*/*z* 459.23709 $[M+H]^+$ (calcd. for $C_{26}H_{35}O_7$, 459.23773).

Hemiacetalmeroterpenoid B (**2**): white powder, m.p. 106.9–108.4 °C; $[\alpha]_D^{25}$ −56 (*c* 0.02, MeOH), UV (MeOH) λ_{max} (log ε): 205 (2.83), 238 (1.36) (Figure S34); ECD (MeOH) λ_{max} ($\Delta\varepsilon$): 206 (−11.92), 248 (+3.38), 311 (−1.19); ^{1}H (600 MHz, CD_3OD) and ^{13}C NMR (150 MHz, CD_3OD) data, see Table 1; HR-ESI-MS: *m*/*z* 445.25772 $[M+H]^+$ (calcd. for $C_{26}H_{37}O_6$, 445.25847).

Hemiacetalmeroterpenoid C (**3**): white powder, m.p. 100.8–102.6 °C; $[\alpha]_D^{25}$ −66 (*c* 0.02, MeOH), UV (MeOH) λ_{max} (log ε): 205 (2.51), 260 (1.78) (Figure S35); ECD (MeOH) λ_{max} ($\Delta\varepsilon$): 206 (−18.31), 240 (+12.72), 310 (−2.18); ^{1}H (600 MHz, CD_3OD) and ^{13}C NMR (150 MHz, CD_3OD) data, see Table 1; HR-ESI-MS: *m*/*z* 509.25015 $[M+Na]^+$ (calcd. for $C_{28}H_{38}O_7Na$, 509.25097).

Astellolide J (**14**): yellow powder, m.p. 202.9–204.5 °C; $[\alpha]_D^{25}$ +16 (*c* 0.02, MeOH), UV (MeOH) λ_{max} (log ε): 216 (3.15) (Figure S36); ECD (MeOH) λ_{max} ($\Delta\varepsilon$): 203 (−1.82), 225 (+3.27); ^{1}H (400 MHz, CD_3OD) and ^{13}C NMR (100 MHz, CD_3OD) data; HR-ESI-MS: *m*/*z* 305.13565 $[M+Na]^+$ (calcd. for $C_{15}H_{22}O_5Na$, 305.13594).

Astellolide Q (**15**): yellow powder, m.p. 160.1–162.2 °C; $[\alpha]_D^{25}$ +12 (*c* 0.02, MeOH), UV (MeOH) λ_{max} (log ε): 218 (3.62) (Figure S37); ECD (MeOH) λ_{max} ($\Delta\varepsilon$): 232 (+5.19); ^{1}H (400 MHz, CD_3OD) and ^{13}C NMR (100 MHz, CD_3OD) data, see Table 2; HR-ESI-MS: *m*/*z* 347.14578 $[M+Na]^+$ (calcd. for $C_{17}H_{24}O_6Na$, 347.14578).

3.5. ECD Calculation

Firstly, ECD calculations of compounds **1**–**3** and **14**–**15** were performed by the Gaussian 09 program and Spartan'14. Next, the conformations with a Boltzmann population (>5%) were selected for optimization and calculation in methanol at B3LYP/6-31+G (d, p). Finally, the ECD spectra were generated by the program SpecDis 1.6 (University of Würzburg, Würzburg, Germany) and drawn by OriginPro 8.0 (OriginLab, Ltd., Northampton, MA, USA) from dipole-length rotational strengths by applying Gaussian band shapes with sigma = 0.30 eV [29,30].

3.6. Bioassays Antimicrobial Activity

Antimicrobial activity assay was performed as previously described in [31,32].

4. Conclusions

In summary, three new andrastin-type meroterpenoids (**1**–**3**), one new drimane sesquiterpenoid (**15**) and one sesquiterpenoid J (**14**) that was first isolated from a natural source, together with ten known compounds (**4**–**13**) were isolated from the cultures of the rhizosphere soil of mangrove plant *Avicennia marina* fungus *Penicillium* sp. N-5. Their structures were determined by the analysis of NMR, HR-MS and ECD spectra. All the isolated compounds were investigated for their antimicrobial activities against two phytopathogenic fungi and four bacterial strains. Among them, compounds **1**, **5** and **10** exhibited significant inhibition against *Penicillium italicum* and *Colletrichum gloeosporioides* with MIC values of 6.25, 1.56, 6.25 and 6.25, 3.13, 6.25 μg/mL. Notably, compound **5** showed potential antimicrobial activity against all the strains and the MIC values were lower than 25 μg/mL. Moreover, andrastin-type meroterpenoid antimicrobial activity against phytopathogenic fungi was reported for the first time.

Supplementary Materials: The following are available online at https://www.mdpi.com/article/10.3390/md20080514/s1, Figure S1: HRESIMS spectrum of compound **1**; Figure S2: ^{1}H NMR spectrum of compound **1**; Figure S3: ^{13}C NMR spectrum of compound **1**; Figure S4: DEPT135 spectrum of compound **1**; Figure S5. HSQC spectrum of compound **1**; Figure S6: H, H-COSY spectrum of compound **1**; Figure S7: HMBC spectrum of compound **1**; Figure S8: NOE spectrum of compound **1**; Figure S9: HRESIMS spectrum of compound **2**; Figure S10: ^{1}H NMR spectrum of compound **2**; Figure S11: ^{13}C NMR spectrum of compound **2**; Figure S12: DEPT135 spectrum of compound **2**; Figure S13: HSQC spectrum of compound **2**; Figure S14: H, H-COSY spectrum of compound **2**; Figure S15: HMBC spectrum of compound **2**; Figure S16: NOE spectrum of compound **2**; Figure S17: HRESIMS spectrum of compound **3**; Figure S18: ^{1}H NMR spectrum of compound **3**; Figure S19: ^{13}C NMR spectrum of compound **3**; Figure S20: HSQC spectrum of compound **3**; Figure S21: H, H-COSY spectrum of compound **3**; Figure S22: HMBC spectrum of compound **3**; Figure S23: NOE spectrum of compound **3**; Figure S24: NOE spectrum of compound **14**; Figure S25: HRESIMS spectrum of compound **15**; Figure S26: ^{1}H NMR spectrum of compound **15**; Figure S27: ^{13}C NMR spectrum of compound **15**; Figure S28. DEPT135 spectrum of compound **15**; Figure S29: HSQC spectrum of compound **15**; Figure S30: H, H-COSY spectrum of compound **15**; Figure S31: HMBC spectrum of compound **15**; Figure S32: NOE spectrum 3M of compound **15**; Figure S33: UV and ECD of compound **1**; Figure S34: UV and ECD of compound **2**; Figure S35: UV and ECD of compound **3**; Figure S36: UV and ECD of compound **14**; Figure S37: UV and ECD of compound **15**.

Author Contributions: T.C. performed the experiments and wrote the paper; W.Y. analyzed the data and discussed the results; T.L., Y.Y. and Y.L. participated in the experiments; B.W. and Z.S. reviewed the manuscript; Z.S. designed and supervised the experiments. All authors have read and agreed to the published version of the manuscript.

Funding: We thank the National Natural Science Foundation of China (U20A2001, 21877133), GDNRC [2022]35 and the Key-Area Research and Development Program of Guangdong Province (2020B1111030005) for their generous support.

Institutional Review Board Statement: Not applicable.

Informed Consent Statement: Not applicable.

Data Availability Statement: Data are contained within the article and Supplementary Material.

Conflicts of Interest: The authors declare no conflict of interest.

References

1. Matsuda, Y.; Quan, Z.; Mitsuhashi, T.; Li, C.; Abe, I. Cytochrome P450 for citreohybridonol synthesis: Oxidative derivatization of the andrastin scaffold. *Org. Lett.* **2016**, *18*, 296–299. [CrossRef] [PubMed]
2. Matsuda, Y.; Awakawa, T.; Abe, I. Reconstituted biosynthesis of fungal meroterpenoid andrastin A. *Tetrahedron* **2013**, *69*, 8199–8204. [CrossRef]
3. Cheng, X.; Liang, X.; Zheng, Z.H.; Zhang, X.X.; Lu, X.H.; Yao, F.H.; Qi, S.H. Penicimeroterpenoids A-C, meroterpenoids with rearrangement skeletons from the marine-derived fungus *Penicillium* sp. SCSIO 41512. *Org. Lett.* **2020**, *62*, 6330–6333. [CrossRef]
4. Qin, Y.Y.; Huang, X.S.; Liu, X.B.; Mo, T.X.; Xu, Z.L.; Li, B.C.; Qin, X.Y.; Li, J.; Schäberle, T.F.; Yang, R.Y. Three new andrastin derivatives from the endophytic fungus *Penicillium vulpinum*. *Nat. Prod. Res.* **2022**, *36*, 13. [CrossRef] [PubMed]
5. Ren, J.; Huo, R.; Liu, G.; Liu, L. New andrastin-type meroterpenoids from the marine-derived fungus *Penicillium* sp. *Mar. Drugs* **2021**, *19*, 189. [CrossRef]
6. Xie, C.L.; Xia, J.M.; Lin, T.; Lin, Y.J.; Lin, Y.K.; Xia, M.L.; Chen, H.F.; Luo, Z.H.; Shao, Z.Z.; Yang, X.W. Andrastone A from the deep sea-derived fungus *Penicillium allii-sativi* acts as an inducer of caspase and RXRa-dependant apoptosis. *Front. Chem.* **2019**, *7*, 692. [CrossRef] [PubMed]
7. Cheng, Z.; Xu, W.; Wang, Y.; Bai, S.; Liu, L.; Luo, Z.; Yuan, W.; Li, Q. Two new meroterpenoids and two new monoterpenoids from the deep sea-derived fungus *Penicillium* sp. YPGA11. *Fitoterapia* **2019**, *133*, 120–124. [CrossRef] [PubMed]
8. Powers, Z.; Scharf, A.; Cheng, A.; Yang, F.; Himmelbauer, M.; Mitsuhashi, T.; Barra, L.; Taniguchi, Y.; Kikuchi, T.; Fujita, M.; et al. Biomimetic synthesis of meroterpenoids by dearomatization-driven polycyclization. *Angew. Chem. Int. Ed.* **2019**, *58*, 16141–16146. [CrossRef] [PubMed]
9. Zong, Y.; Wang, W.J.; Xu, T. Total synthesis of bioactive marine mero-terpenoids: The cases of liphagal and frondosin B. *Mar. Drugs* **2018**, *16*, 115. [CrossRef] [PubMed]
10. Kuan, K.K.W.; Markwell-Heys, A.W.; Cruickshank, M.C.; Tran, D.P.; Adlington, R.M.; Baldwin, J.E.; George, J.H. Biomimetic synthetic studies on meroterpenoids from the marine sponge *Aka coralliphaga*: Divergent total syntheses of siphonodictyal B, liphagal and corallidictyals A–D. *Bioorgan. Med. Chem.* **2019**, *27*, 2449–2465. [CrossRef] [PubMed]

11. Wang, W.; Shi, Y.; Liu, Y.; Zhang, Y.; Wu, J.; Zhang, G.; Che, Q.; Zhu, T.; Li, M.; Li, D. Brasilterpenes A-E, bergamotane sesquiterpenoid derivatives with hypoglycemic activity from the deep sea-derived fungus *Paraconiothyrium brasiliense* HDN15-135. *Mar. Drugs* **2022**, *20*, 338. [CrossRef]
12. Chen, S.; Cai, R.; Liu, Z.; Cui, H.; She, Z. Secondary metabolites from mangrove-associated fungi: Source, chemistry and bioactivities. *Nat. Prod. Rep.* **2022**, *39*, 560. [CrossRef]
13. Zhao, Y.; Sun, C.; Huang, L.; Zhang, X.; Zhang, G.; Che, Q.; Li, D.; Zhu, T. Talarodrides A-F, nonadrides from the antarctic sponge-derived fungus *Talaromyces* sp. HDN1820200. *J. Nat. Prod.* **2021**, *84*, 3011–3019. [CrossRef]
14. Shun, C.; Liu, Q.; Shah, M.; Che, Q.; Zhang, G.; Zhu, T.; Zhou, J.; Rong, X.; Li, D. Talaverrucin A, heterodimeric oxaphenalenone from antarctica sponge-derived fungus *Talaromyces* sp. HDN151403, Inhibits Wnt/β-Catenin Signaling Pathway. *Org. Lett.* **2022**, *24*, 3993–3997. [CrossRef]
15. Ye, G.; Huang, C.; Li, J.; Chen, T.; Tang, J.; Liu, W.; Long, Y. Isolation, structural characterization and antidiabetic activity of new diketopiperazine Alkaloids from mangrove endophytic fungus *Aspergillus* sp. 16-5c. *Mar. Drugs* **2021**, *19*, 402. [CrossRef]
16. Wu, Q.; Chang, Y.; Che, Q.; Li, D.; Zhang, G.; Zhu, T. Citreobenzofuran D-F and phomenone A-B: Five novel sesquiterpenoids from the mangrove-derived fungus *Penicillium* sp. HDN13-494. *Mar. Drugs* **2022**, *20*, 137. [CrossRef]
17. Yang, W.; Tan, Q.; Yin, Y.; Chen, Y.; Zhang, Y.; Wu, J.; Gao, L.; Wang, B.; She, Z. Secondary metabolites with α-glucosidase inhibitory activity from mangrove endophytic fungus *talaromyces* sp. CY-3. *Mar. Drugs* **2021**, *19*, 492. [CrossRef]
18. Zang, Z.; Yang, W.; Cui, H.; Cai, R.; Li, C.; Zou, G.; Wang, B.; She, Z. Two antimicrobial heterodimeric tetrahydroxanthones with a 7, 7′-Linkage from mangrove endophytic fungus *Aspergillus flavus* QQYZ. *Molecules* **2022**, *27*, 2691. [CrossRef]
19. Zou, G.; Chen, Y.; Yang, W.; Zang, Z.; Jiang, H.; Chen, S.; Wang, B.; She, Z. Furobenzotropolones A, B and 3-Hydroxyepicoccone B with antioxidative activity from mangrove endophytic fungus *Epicoccum nigrum* MLY-3. *Mar. Drugs* **2021**, *19*, 395. [CrossRef]
20. Chen, Y.; Yang, W.; Zou, G.; Wang, G.; Kang, W.; Yuan, J.; She, Z. Cytotoxic bromine- and iodine-containing cytochalasins produced by the mangrove endophytic fungus *Phomopsis* sp. QYM-13 using the OSMAC approach. *J. Nat. Prod.* **2022**, *85*, 1229–1238. [CrossRef]
21. Jiang, H.; Cai, R.; Zang, Z.; Yang, W.; Wang, B.; Zhu, G.; Yuan, J.; She, Z. Azaphilone derivatives with anti-inflammatory activity from the mangrove endophytic fungus *Penicillium sclerotiorum* ZJHJJ-18. *Bioorg. Chem.* **2022**, *122*, 105721. [CrossRef] [PubMed]
22. Cai, R.; Jiang, H.; Xiao, Z.; Cao, W.; Yan, T.; Liu, Z.; Lin, S.; Long, Y.; She, Z. (−)- and (+)-Asperginulin A, a pair of indole diketopiperazine alkaloid dimers with a 6/5/4/5/6 pentacyclic skeleton from the mangrove endophytic fungus *Aspergillus* sp. SK-28. *Org. Lett.* **2019**, *21*, 9633–9636. [CrossRef] [PubMed]
23. Gao, S.S.; Shang, Z.; Li, X.M.; Li, C.S.; Gui, C.M.; Wang, B.G. Secondary metabolites produced by solid fermentation of the marine-derived fungus *Penicillium commune* QSD-17. *Biosci. Biotechnol. Biochem.* **2012**, *76*, 358–360. [CrossRef] [PubMed]
24. Kosemura, S.H.; Miyata, K.; Matsunaga, S. Yamamura, Biosynthesis of citreohybridones, the metabolites of a hybrid strain KO 0031 derived from *penicillium citreo-viride* B. IFO 6200 and 4692. *Tetrahedron Lett.* **1992**, *33*, 3883–3886. [CrossRef]
25. Shiomi, K.R.; Uchida, J.; Inokoshi, H.; Tanaka, Y.; Iwai, S. Ōmura, Andrastins A-C, new protein farnesyltransferase inhibitors, produced by *Penicillium* sp. FO-3929. *Tetrahedron Lett.* **1996**, *37*, 1265–1268. [CrossRef]
26. Yang, X.; Xie, C.; Xia, J.; He, Z. Andrastone Compound and its Preparation Method and Application in Preparation of Antiallergic Drug. CN 111217878, 2 June 2020.
27. Hamasaki, T.; Kuwano, H.; Isono, K.; Hatsuda, Y.; Fukuyama, K.; Tsukihara, T.; Katsube, Y. A new metabolite, parasiticolide A, from *Aspergillus parasiticus*. *Agric. Biol. Chem.* **1975**, *37*, 749–751. [CrossRef]
28. Kosemura, S. Meroterpenoids from *Penicillium citreo-viride* B. IFO 4692 and 6200 hybrid. *Tetrahedron* **2003**, *59*, 5055–5072. [CrossRef]
29. Cui, H.; Liu, Y.N.; Li, J.; Huang, X.S.; Yan, T.; Cao, W.H.; Liu, H.J.; Long, Y.H.; She, Z.G. Diaporindenes A-D: Four unusual 2,3-dihydro-1H-indene analogues with anti-inflammatory activities from the mangrove endophytic fungus *Diaporthe* sp. SYSU. *J. Org. Chem.* **2018**, *83*, 11804–11813. [CrossRef]
30. Frisch, M.J.; Trucks, G.W.; Schlegel, H.B.; Scuseria, G.E.; Robb, M.A.; Cheeseman, J.R.; Scalmani, G.; Barone, V.; Mennucci, B.; Petersson, G.A.; et al. *Gaussian 09*; Gaussian, Inc.: Wallingford, UK, 2016.
31. Yang, W.; Yuan, J.; Tan, Q.; Chen, Y.; Zhu, Y.; Jiang, H.; Zou, G.; Zang, Z.; Wang, B.; She, Z. Peniazaphilones A-I, produced by co-culturing of mangrove endophytic fungi, *Penicillium sclerotiorum* THSH-4 and *Penicillium sclerotio-rum* ZJHJJ-18. *Chin. J. Chem.* **2021**, *39*, 3404–3412. [CrossRef]
32. Chen, Y.; Yang, W.; Zou, G.; Chen, S.; Pang, J.; She, Z. Bioactive polyketides from the mangrove endophytic fungi *Phoma* sp. SYSU-SK-7. *Fitoterapia* **2019**, *139*, 10436. [CrossRef]